



Electromagnetic energy absorption potential and microwave heating capacity of SiC thin films in the 1–16 GHz frequency range

B. Aïssa^{a,d,*}, N. Tabet^b, M. Nedil^c, D. Therriault^d, F. Rosei^e, R. Nechache^{e,f}

^a Department of Smart Materials and Sensors for Space Missions, MPB Technologies Inc., 151 Hymus Boulevard, Montreal, H9R 1E9, Canada

^b Physics Department, Center of Excellence in Nanotechnology (CENT), PO 477, KFUPM, Saudi Arabia

^c Laboratoire de Recherche Télébec en Communications Souterraines, UQAT, 450, 3e Avenue, Val-d'Or J9P 1S2, Canada

^d Center for Applied Research on Polymers (CREPEC), Mechanical Engineering Department, École Polytechnique de Montréal, PO Box 6079, Montreal, H3C 3A7, Canada

^e Centre Énergie, Matériaux et Télécommunications, INRS, 1650, Boulevard Lionel-Boulet, Varennes, Quebec J3X 1S2, Canada

^f NAST Center and Department of Chemical Science and Technology, University of Rome Tor Vergata, 00133 Rome, Italy

ARTICLE INFO

Article history:

Received 5 January 2012

Received in revised form 10 February 2012

Accepted 12 February 2012

Available online 20 February 2012

Keywords:

PECVD

Silicon carbide materials

EM absorption

Microwave heating

ABSTRACT

We report on the electromagnetic (EM) absorption potential and microwave heating capacity of amorphous hydrogenated silicon carbide thin films (a-SiC:H) in the 1–16 GHz frequency domain. a-SiC:H thin films with typical thickness of 1 μm were deposited by plasma enhanced chemical vapor deposition on [100] undoped silicon substrates, and exhibit a deep EM absorption – up to 96% of the total EM energy irradiation – which is systematically converted into heat. Two-wavelength pyrometer tests show that temperatures exceeding 2000 K can be reached in a very short time, less than 100 s exposure to microwaves, showing a promising potential for specific microwave heating applications.

© 2012 Elsevier B.V. All rights reserved.

1. Introduction

Amorphous silicon carbide (a-SiC) is an attractive semiconducting material since its wide band gap ranges from 1.8 to 2.6 eV, when the carbon content in the material varies. a-SiC has outstanding physical and chemical characteristics, such as high breakdown electric field ($\sim 2.2 \times 10^8$ V/m), high thermal conductivity (~ 380 W/mK) [1] and high electron mobility [2], with very promising applications like protective coatings on microelectromechanical systems (MEMS) [3], barrier layers for organic light emitting diodes [4], solar cells and color sensor [5,6], etc. Plasma-enhanced chemical vapor deposition (PECVD), operating with silane and methane gas mixtures in the so called “low power regime” is one of the most widely employed technique aimed at growing high-quality hydrogenated amorphous silicon carbide (a-SiC:H) [7,8]. On the contrary, the rapid development of advanced electronic devices has brought a growing interest in electromagnetic (EM) wave-absorbing materials [9–11]. Many commercial and military applications, such as data transmission, telecommunications, wireless network systems, and satellite broadcasting, as well

as radars, and diagnostic and detection systems, utilize and emit electromagnetic waves. The interaction of electromagnetic waves originating from different sources can lead to a decrease in quality and a misinterpretation of transferred data, and it has thus become vital to avoid such interference and electromagnetic wave pollution through the use of appropriate absorbing and shielding materials.

Electromagnetic wave-absorbing materials absorb and dissipate electromagnetic energy to which they are exposed, reducing reflected and/or scattered electromagnetic components to a minimum. There are various magnetic materials, such as ferrites, carbonyl iron, cobalt, and their related based composite, which can be used as magnetic absorbers [12–15], with the main drawbacks that they are heavy, and only effective in the MHz frequency range [16,17]. On the contrary, dielectric materials stand out due to their low density and effectiveness in the GHz frequency range. Carbonaceous materials – such as graphite and/or carbon black [16–18] – are often used as dielectric EM absorbers, generating dielectric loss by improving the electrical conductivity of the mixture. In addition, and according to the literature data, thick silicon carbide nanowires [19], SiC powder [20] and/or Ni–Co–P-coated SiC powder [21] have also shown a high wave absorption ability, where the reflection loss of a Ni–Co–P-coated SiC micrometer particle, for example, was found to reach sometimes the value of “–30 dB” [21] (which is attributed mainly to the magnetization of Co and Ni metals). Moreover, SiC short fibers [22] or SiC-based ceramic woven fabrics [23] were deeply investigated and demonstrated to be good

* Corresponding author at: Department of Smart Materials and Sensors for Space Missions, MPB Technologies Inc., 151 Hymus Boulevard, Montreal, H9R 1E9, Canada. Tel.: +1 514 694 8751; fax: +1 514 695 7492.

E-mail address: aissab@emt.inrs.ca (B. Aïssa).

candidate materials for EM wave absorption applications. As a matter of fact, the average of reflection loss of SiC-based ceramic micrometer fibers was found about “–10 dB” at 17 GHz frequency [23].

In this work, we study the electromagnetic wave-absorbing capacity of PECVD grown a-SiC:H thin films with typical thickness of 1 μm . A deep EM absorption (EMA) – up to $|-14|$ dB which represents more than 96% of the total EM energy irradiation – was recorded in the 1–16 GHz frequency domain, and was found to be systematically converted into heat. By using the two-wavelength pyrometer tests, we have shown that temperatures exceeding 2000 K can be reached in a very short time, less than 100 s exposure to microwaves, showing a promising potential for specific microwave heating applications.

2. Experimental

a-SiC:H films were deposited by standard commercially available parallel plate capacitance PECVD tools, using silane and methylsilane like sources. The total gas flow rate was 24 sccm (standard cubic centimetres per minute), with a total chamber pressure kept constant at 300 mbar using downstream pressure control. All films were deposited on 3 in. [100] undoped silicon substrates (500 nm-thick) at temperatures in the order of 400 °C. A radio frequency density of 0.345 W/cm² at 100 kHz, and ultra high purity (UHP) argon (99.999%) gas were used (the ratio between source gas and dilution gas argon was kept at 1:8). Hydrogenated a-SiC:H films of typically $\sim 1 \mu\text{m}$ thicknesses were then exposed to 2.45 GHz EM irradiation at 900 W power energy, for various exposure times, ranging from 10 to 300 s. It's worth noting that the quality of the SiC films is known to be highly influenced by the deposition parameters [24,25].

The Raman scattering spectra of the a-SiC films were performed with the 514.5 nm (2.41 eV) laser radiation of an Ar⁺ laser focused onto the sample with a spot of 1 μm (microRaman spectroscopy, Renishaw Imaging Microscope WireTM). The Raman spectra were taken with a backscattering geometry at room temperature in the 300–600 cm⁻¹ region. The Raman peak positions were calibrated using more than six high-resolution measurements performed for every sample, achieving 0.1–0.2 cm⁻¹ accuracy in terms of the relative position measurement. The bonding configurations were measured by Fourier transform infrared spectroscopy, FTIR (Nicolot AVATAR 360). The as-deposited and the EM irradiated a-SiC specimens were characterized by using contact mode atomic force microscopy, AFM (NanoScope III, Digital Instrument) operated at room temperature in ambient air.

The microwave heating of the a-SiC sample specimen was monitored as a function of its EM exposure time by means of a two-wavelength pyrometer (Metis MQ22) connected to a computer. The two wavelength pyrometer presents the main advantage of avoiding the uncertainties on the temperature measurements related to the thermal emissivity of the heated target.

3. Results and discussion

Fig. 1 shows the evolution of the measured temperature (i.e., microwave heating), with respect to the exposure time to EM irradiation, at 2.45 GHz frequency and EM power of 900 W. It can be observed that in all tests, a temperature equal to 1173 K (which is the minimum temperature measured by the pyrometer) was reached after about only 40 s exposure. The microwave heating temperature increases then rapidly and exceeds 1900 K in less than 75 s, and reaches values as high as 2100 K after only 120 s. The microwave heating then saturates around this temperature plateau for the remaining period of EM irradiation test (i.e., until 300 s).

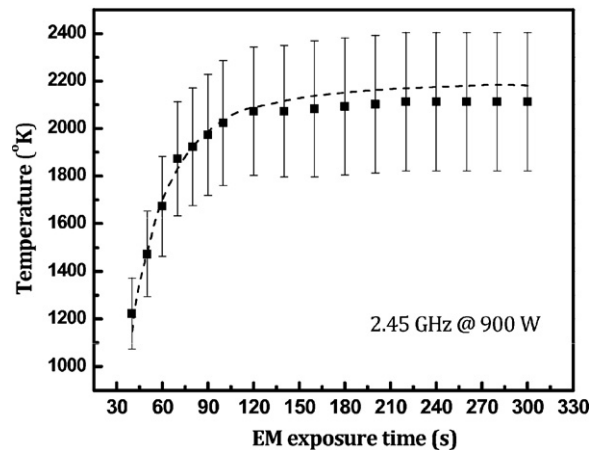


Fig. 1. Evolution of the a-SiC:H thin films microwave heating (at 900 W and 2.45 GHz) as a function of the EM irradiation exposure time, as measured by the two-wavelength pyrometer tests.

In this specific SHF domain (i.e., 1–16 GHz), the EM absorption is primarily due to the existence of permanent Si–C dipole molecules which tend to re-orient under the influence of a microwave electric field. This re-orientation loss mechanism originates from the inability of the polarization to follow extremely rapid reversals of the electric field (i.e., at 2.45 GHz). At such high frequencies therefore, the resulting polarization phasor lags the applied electric field. This ensures that the resulting current density has a component in phase with the EM field, and therefore power is dissipated in the SiC material as microwave heating.

The EM properties of the a-SiC:H films were characterized by using the coaxial transmission line method [26]. To verify the EM-attenuation feature of the films, measurements of the EM energy transfer in a transition device were performed (holder adapter). The mentioned transition uses EM coupling through a slot etched in a common ground plane between two ports, one based on conductor backed coplanar waveguide technology, and another based on micro-strip technology. The transition structure is characterized by a wide-band operating in the 1–16 GHz frequency range [27]. To measure the transition scattering parameters, an Agilent 8722ES network analyzer was used. For each setup, transmission (S_{21}) and reflection (S_{11}) parameters were recorded with the network analyzer. The EM attenuation is deduced by comparing energy transmission between the two ports of the transition device in cases with and without measured samples.

The holder adapter, the reference silicon sample, and the a-SiC:H thin films specimen (in both conditions, i.e., as-grown and after its EM exposure for 300 s and hence its microwave heating) exhibit a reflection coefficient of more than $|-70|$ dB around the 9 GHz frequency (Fig. 2(a)), which means that less than 10^{-7} fraction of the incident EM energy was reflected, meaning that no EM reflection occurs at this frequency domain, and that the whole EM energy is then transmitted from the coaxial cable to the a-SiC specimen under test. The EM absorption (and/or attenuation, (S_{21})) of the a-SiC thin films samples was systematically measured with respect to the frequency. As seen in Fig. 2(b), the holder adapter and reference silicon substrate are almost transparent to EM radiation in the investigated frequency range. However, a deep EM-attenuation, with a (S_{21}) reaching up to $|-14|$ dB is measured for a-SiC thin films (no significant difference was noted in both cases, before and after EM exposure). This demonstrates as well that, at this frequency domain, the predominant EM attenuation mechanism in a-SiC thin films is absorption rather than reflection.

Fig. 3(a) shows typical AFM images of the as grown a-SiC thin films, having a RMS roughness of 0.51 nm. The AFM image of the

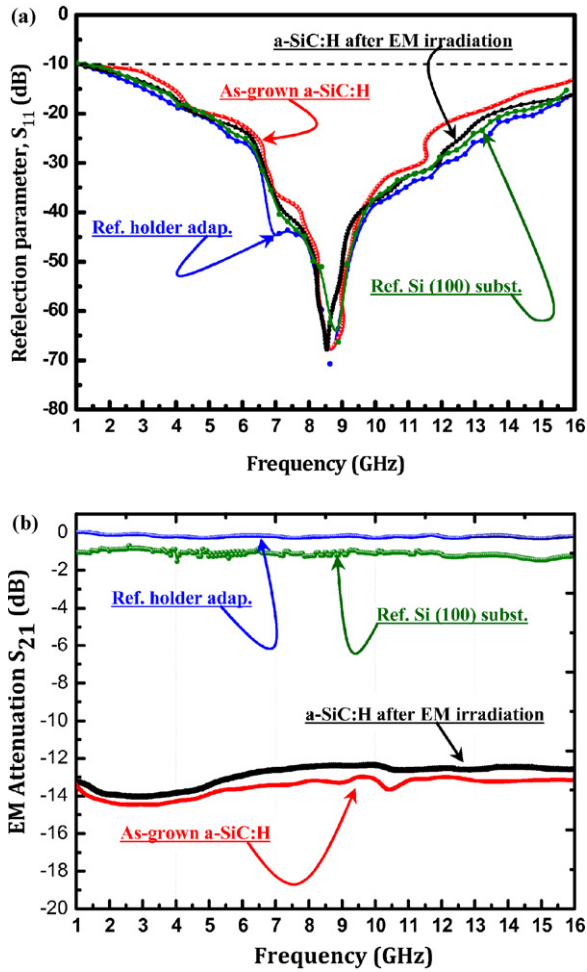


Fig. 2. (a) The reflection parameter (S_{11}) and (b) EM absorption parameter (S_{21}) measured for the holder adapter, the naked reference Si (100) substrate, and the as-grown and EM irradiated a-SiC thin films, respectively.

same sample after its exposure to EM irradiation for 300 s – and then its microwave heating up to 2100 K – is shown in Fig. 3(b), where the roughness was found to increase almost 5 times (RMS up to 2.52 nm) comparatively to the as-grown SiC films. It can be also seen the formation of small SiC nanoparticles (NPs) at the top of

the SiC films, happening after the microwave heating process. This is highly likely due to the annealing temperature resulting from EM irradiation, inducing the cracking of the a-SiC films and the formation of NPs. These NPs were found to be uniformly distributed onto the SiC films surface. Their representative distribution sizes were determined from topographic heights in the AFM image and their associated distribution histogram (fitted with a Gaussian distribution and giving a NPs mean size of 2.65 ± 0.65 nm) is shown in Fig. 3(c).

To obtain more information about the structural properties of the a-SiC thin films, microRaman spectroscopy was used. Indeed, since the pioneering work of Anastassakis et al. [28] who have performed, for the first time, an experimental investigation of the effects of static uniaxial stress of silicon by means of Raman spectroscopy, this technique became increasingly popular for local mechanical stress measurements (the theory underlying the Raman spectroscopy for local mechanical stress in silicon integrated circuits can be found well detailed in Ref. [29] as well). Moreover, Raman spectroscopy is known to be one of the best methods to characterize identical atomic polar bonds, such as Si–Si and C–C bonds. The Raman spectra from these samples are characterized by the presence of bonds characteristic of amorphous material in the $300\text{--}600\text{ cm}^{-1}$ spectral region. As shown in Fig. 4(a), for the as-grown a-SiC sample, the transverse optical (TO) band of polycrystalline Si (100) peak appears at 520 cm^{-1} due to the transparent nature at the high band gap a-SiC films. After EM absorption, this characteristic peak is shifted to higher wave numbers, suggesting that tensile stresses are observed in the silicon areas which increase as the temperature (i.e., heating) increases.

The FTIR is also a powerful tool to investigate the bonding structure in a-SiC films. All spectra were collected in transmission mode and the Si substrate background was subtracted by pre-scanning a bare Si wafer and subtracting the resulting spectrum from that of the a-SiC:H/Si sample. Scans were made from 400 to 2200 cm^{-1} with a resolution of 2 cm^{-1} and averaged over ten scans. Representative FTIR absorption spectra for a-SiC films before and after their EM exposure are shown in Fig. 4(b). It can be seen that the measured spectra are characterized by an absorption peak related to the Si–C bond, which occurs at around 800 cm^{-1} . Compared with as-grown a-SiC sample, the full width at half maximum (FWHM) of the band around 800 cm^{-1} in sample after its EM exposure is narrower (304 instead of 341 cm^{-1}). This result suggests strongly that the stoichiometric proportion of the SiC film is most probably improved, and a higher-quality SiC films could be obtained after their EM absorption and microwave heating. Moreover, the Si–C peak is shifted to

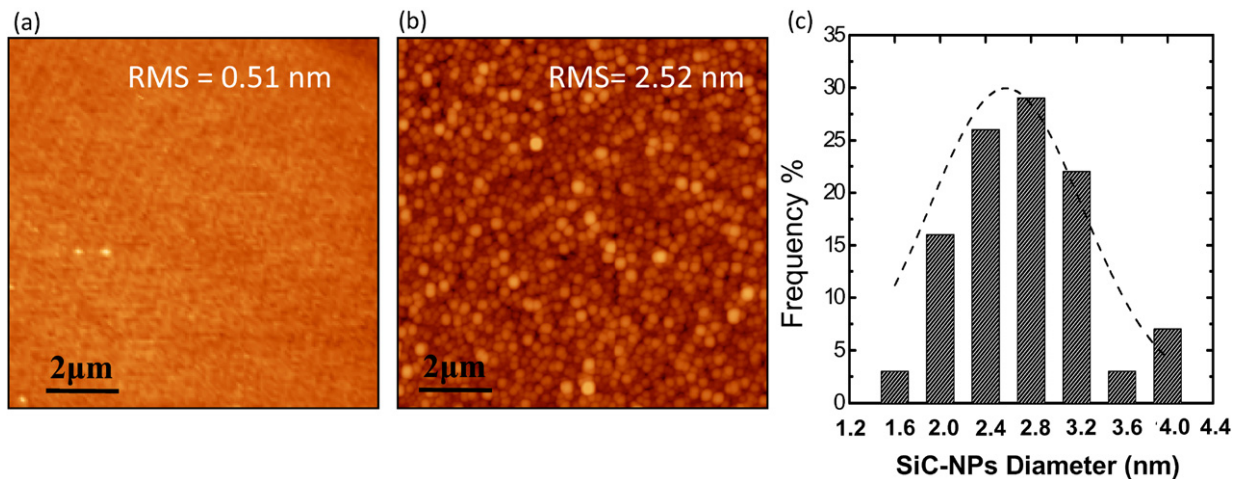


Fig. 3. Typical AFM image of a-SiC:H thin films, (a) as-grown and (b) after its EM exposure for 300 s (and/or their microwave heating), (c) shows the histogram of the size distribution of the formed SiC-NPs after microwave heating.

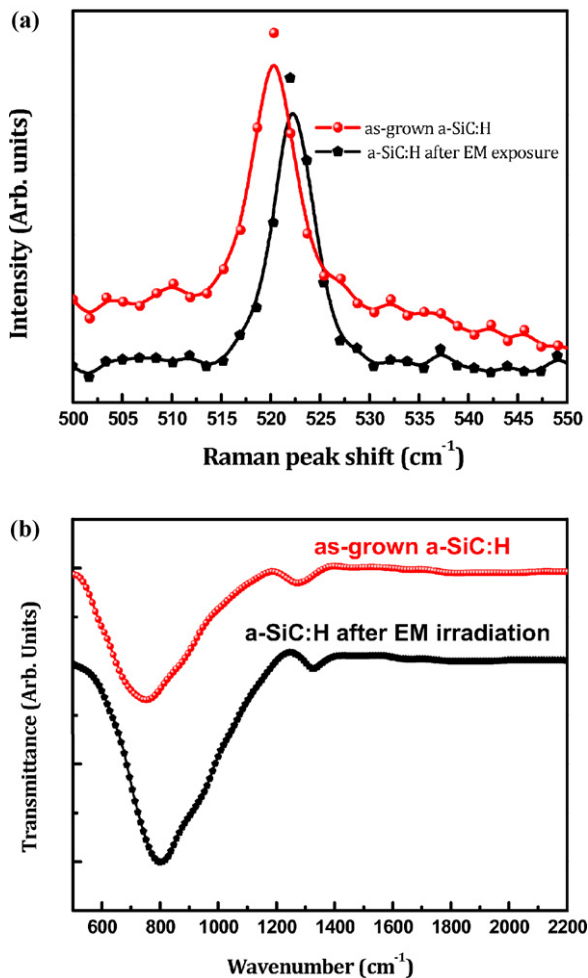


Fig. 4. (a) microRaman scattering, (b) FTIR measurements spectra of the as grown and microwave heated a-SiC films (300 s EM exposure), respectively.

higher wave numbers. This can be attributed as well to a decrease in the length of the Si–C bonds as there is compressive strain in the thin films and is possibly associated with the formation of nanostructures (i.e., NPs) in the SiC films after the EM exposure. A similar shift has been reported and attributed to the progressively larger size of the precipitates NPs of SiC [30], or the increasing stoichiometry of $\text{Si}_{1-x}\text{C}_x$ in the films [31]. However, to correlate the Raman/FTIR results with the Si/C concentrations ratios (and hence the chemical composition) into the a-SiC:H films, detailed analysis and/or characterizations are required, particularly, the Rutherford backscattering (RBS) measurements coupled with Auger electron spectroscopy (AES), while the resonant nuclear reaction method is well suitable for the hydrogen content determination.

4. Conclusions

In conclusion, the electromagnetic wave absorption capacity of a-SiC:H thin films was determined in the 1–16 GHz frequency range using the coaxial transmission line method. Our results have shown a systematic and deep EM absorption –up to 96% of the total microwave EM energy irradiation–, which is converted into heat, as measured by two-wavelength pyrometer tests. Temperatures exceeding 2000 K were reached in very short time, less than 100 s exposure to microwaves. Our results show a promising potential for using a-SiC materials as specific microwave absorbers and fast microwave heater applications.

Acknowledgments

We acknowledge financial support from the Canada Foundation for Innovation, the Natural Science and Engineering Research Council (NSERC) of Canada, the Fonds Québécois de la Recherche sur la Nature et les Technologies (FQRNT). F.R. is grateful to the Canada Research Chairs Program for partial salary support and to MDEIE for an international collaboration grant with the University of Rome “Tor Vergata”.

Appendix A.

The main purpose of EM shielding is to create a barrier that attenuates radiated electromagnetic energy through reflection and/or absorption. EMA is a measurement of electromagnetic signal attenuation after a shield is introduced. EMA accounts for the shielding due to both absorption (S_{21}) and reflection (S_{11}) [32]. The EMA is defined in terms of the power ratio of the incident and transmitted EM wave as follows:

$$\text{EM}_{\text{abs}} = 10 \log \frac{P_I}{P_T} = 20 \log \frac{E_I}{E_T}$$

where $P_I(E_I)$ and $P_T(E_T)$ are the power (EM field) of the incident and transmitted EM waves, respectively [33]. The unit of the EM shielding is decibel (dB).

References

- [1] S. Hu, K. Sheng, *Solid State Electron.* 48 (2004) 1861.
- [2] J. Seo, S. Yoon, K. Miihara, K. Kim, *Thin Solid Films* 406 (2002) 138.
- [3] H. Zhang, H. Guo, Y. Wang, G. Zhang, Zh Li, J. *Micromech. Microeng.* 17 (2007) 426.
- [4] L. Zambov, K. Weidner, V. Shamamian, R. Camilletti, U. Pernisz, M. Loboda, G. Cerny, D. Gidley, H.-G. Peng, R. Vallery, *J. Vac. Sci. Technol. A* 24 (2006) 1706.
- [5] Y. Tawada, M. Kondo, H. Okamoto, Y. Hamakawa, *Solar Energy Mater.* 6 (1982) 299.
- [6] B. Lipovšek, A. Jósowskiak, J. Krč, M. Topič, D.M.F. Prazeres, V. Chu, J.P. Conde, A. Joskowiak, *Sens. Actuators A Phys.* 163 (2010) 96.
- [7] I. Solomon, M.P. Schmidt, H. Tran-Quoc, *Phys. Rev. B* 38 (1988) 9895.
- [8] J. Pereyra, M.N. Carreno, M.H. Tabacniks, R.J. Prado, M.C.A. Fantini, *J. Appl. Phys.* 84 (1998) 2371.
- [9] K. Isoird, M. Lazar, L. Ottaviani, M.L. Locatelli, C. Raynaud, D. Planson, J.P. Chante, *Appl. Surf. Sci.* 184 (2001) 477.
- [10] S.Y. Myong, S.W. Kwon, K.S. Lim, M. Konagai, *Solar Energy Mater. Solar Cells* 85 (2005) 133.
- [11] F. Solzbacher, C. Imawan, H. Steffes, E. Obermeier, M. Eickhoff, *Sens. Actuators B Chem.* 78 (2001) 216.
- [12] Y.B. Feng, T. Qiu, C.Y. Shen, X.Y. Li, *IEEE Trans. Magn.* 42 (2006) 363.
- [13] J. Li, J. Huang, Y. Qin, F. Ma, *Mater. Sci. Eng. B* 138 (2007) 199.
- [14] M.S. Pinho, M.L. Gregori, R.C.R. Nunes, B.G. Soares, *Eur. Polym. J.* 38 (2002) 2321.
- [15] P. Singh, V.K. Babbar, A. Razdan, S.L. Srivastava, R.K. Puri, *Mater. Sci. Eng. B* 67 (1999) 132.
- [16] W.S. Chin, D.G. Lee, *Compos. Struct.* 77 (2007) 457.
- [17] J.-H. Oh, K.-S. Oh, C.-G. Kim, C.-S. Hong, *Compos. B* 35 (2004) 49.
- [18] N. Dishovskiy, M. Grigorova, *Mater. Res. Bull.* 35 (2000) 403.
- [19] S.-C. Chiu, H.-C. Yu, Y.-Y. Li, *J. Phys. Chem. C* 114 (2010) 1947.
- [20] Z.T. Liu, S. Kirihara, Y. Miyamoto, D. Zhang, *J. Am. Ceram. Soc.* 89 (2006) 2492.
- [21] Y.J. Li, R. Wang, F.M. Qi, C.M. Wang, *Appl. Surf. Sci.* 254 (2008) 4708.
- [22] Y. Kagawa, Y. Imahashi, H. Iba, T. Naganuma, K. Matsumura, *J. Mater. Sci. Lett.* 22 (2003) 159.
- [23] E. Tan, Y. Kagawa, A.F. Dericioglu, *J. Mater. Sci.* 44 (2009) 1172.
- [24] L. Wang, J. Xu, T. Ma, W. Li, X. Huang, K. Chen, *J. Alloys Compd.* 290 (1999) 273.
- [25] I.A. Yunaz, K. Hashizume, S. Miyajima, A. Yamada, M. Konagai, *Solar Energy Mater. Solar Cells* 93 (2009) 1056.
- [26] B. Aïssa, L.L. Laberge, M.A. Habib, T.A. Denidni, D. Therriault, M.A. El Khakani, *J. Appl. Phys.* 109 (2011) 084313.
- [27] M. Nedil, T.A. Denidni, A. Djaiz, *Electron. Lett.* 43 (2007) 464.
- [28] E. Anastassakis, A. Pinczuk, E. Burstein, F.H. Pollak, M. Cardona, *Solid State Commun.* 88 (1993) 1053.
- [29] I. De Wolf, *Semicond. Sci. Technol.* 11 (1996) 139.
- [30] Y. Wei, L. Wangbing, H. Li, F. Guangsheng, *J. Phys. D Appl. Phys.* 37 (2004) 3304.
- [31] D. Chandrasekhar, J. McMurrin, David J. Smith, J. Kouvetakis, J.D. Lorentzen, J. Menéndez, *Appl. Phys. Lett.* 72 (1998) 2117.
- [32] N.C. Das, T.K. Chaki, D. Khastgir, A. Chakraborty, *Compos. A* 31 (2000) 1069.
- [33] H.M. Kim, K. Kim, C.Y. Lee, J. Joo, S.J. Cho, H.S. Yoon, D.A. Pejakovic, J.W. Yoo, A.J. Epstein, *Appl. Phys. Lett.* 84 (2004) 589.